Chimeric Forms of Furin and TGN38 Are Transported from the Plasma Membrane to the Trans-Golgi Network via Distinct Endosomal Pathways

William G. Mallet and Frederick R. Maxfield

Department of Biochemistry, Weill Medical College of Cornell University, New York, New York 10021

Abstract. Furin and TGN38 are membrane proteins that cycle between the plasma membrane and the trans-Golgi network (TGN), each maintaining a predominant distribution in the TGN. We have used chimeric proteins with an extracellular Tac domain and the cytoplasmic domain of TGN38 or furin to study the trafficking of these proteins in endosomes. Previously, we demonstrated that the postendocytic trafficking of Tac-TGN38 to the TGN is via the endocytic recycling pathway (Ghosh, R.N., W.G. Mallet, T.T. Soe, T.E. McGraw, and F.R. Maxfield. 1998. *J. Cell Biol.* 142:923–936). Here we show that internalized Tac-furin is delivered to the TGN through late endosomes, bypassing the endocytic recycling compartment. The transport of Tac-furin from late endosomes to the TGN appears to proceed via an efficient, single-pass mechanism. Delivery of Tac-furin but not Tac-TGN38 to the TGN is blocked by nocodazole, and the two pathways are also differentially affected by wortmannin. These studies demonstrate the existence of two independent pathways for endosomal transport of proteins to the TGN from the plasma membrane.

Key words: endocytosis • endosomes • Golgi complex • protease • transport

Upon internalization from the plasma membrane, most solutes, ligands, lipids, and transmembrane proteins enter compartments known as sorting endosomes (Mukherjee et al., 1997). From these endosomes, the predominant pathways transport most membrane proteins and lipids back to the cell surface, whereas soluble species are delivered to late endosomes and lysosomes (Gruenberg and Maxfield, 1995). However, some transmembrane proteins escape the endocytic recycling pathway and are delivered to other intracellular organelles. Among these is a subset of proteins that are targeted to the TGN, including the cation-independent mannose 6-phosphate/insulin-like growth factor II receptor (CI-MPR)[1] (Duncan and Kornfeld, 1988; Jin et al., 1989), metallocarboxypeptidase D (Varlamov and Fricker, 1998), peptidylglycine α-amidating monooxygenase (Milgram et al., 1993), furin (Bosshart et al., 1994; Molloy et al., 1994; Schäfer et al., 1995; Takahashi et al., 1995), and TGN38 (Ladinsky and Howell, 1992; Bos et al., 1993; Reaves et al., 1993). Each of these proteins exhibits a high degree of enrichment in the TGN, in contrast to recycling proteins such as the transferrin receptor which are delivered to the TGN only very inefficiently (Snider and Rogers, 1985; Green and Kelly, 1992).

Endocytic recycling of membrane proteins, such as transferrin receptors in CHO cells, does not require specific sorting motifs (Mayor et al., 1993), and membrane proteins lacking cytoplasmic domains are recycled efficiently (Jing et al., 1990). Under various other circumstances, positive sorting of membrane proteins is required, as for the polarized delivery of membrane proteins to plasma membrane domains of epithelial cells (Matter et al., 1993; Mostov and Cardone, 1995) or the transport of certain receptors to degradative compartments (Miller et al., 1986). The latter postendocytic fate must result from a specific property of the membrane protein, possibly involving active sorting and removal of the protein from the recycling pathway. Sorting out of the recycling pathway may occur at multiple steps. For example, a transmembrane protein may be retained in the sorting endosome as it matures into a late endosome (Salzman and Maxfield, 1988; Dunn and Maxfield, 1992), thereby preventing delivery to the endocytic recycling compartment (ERC). From the late endosome, such a protein could then be transported to the TGN or to a lysosome. Transport from the plasma membrane to the TGN via late endosomes has

Address correspondence to Frederick R. Maxfield, Department of Biochemistry, Weill Medical College of Cornell University, 1300 York Ave., Room E-215, New York, NY 10021. Tel.: (212) 746-6405. Fax: (212) 746-8875. E-mail: frmaxfie@mail.med.cornell.edu

1. *Abbreviations used in this paper:* CI-MPR, receptor for insulin-like growth factor II and mannose 6-phosphate containing ligands; ERC, endocytic recycling compartment; LDL, low density lipoprotein; PACS-1, phosphofurin acidic cluster sorting protein 1; PI3 kinase, phosphatidylinositol 3-OH kinase.

been proposed for the CI-MPR (Dahms et al., 1989), although this has not been directly demonstrated. Alternatively, a membrane protein may enter the recycling compartment, but then be delivered to the TGN rather than recycling to the plasma membrane. The existence of this pathway is supported by the detection of the small GTPase Rab11 on both the recycling compartment and the TGN (Úrbe et al., 1993; Ullrich et al., 1996) and by the close spatial apposition of the two compartments in many cell types (Hopkins and Trowbridge, 1983; Yamashiro et al., 1984; Lippincott-Schwartz et al., 1991). It is also possible that a pathway directly links sorting endosomes to the TGN, whereby a transmembrane protein could enter the TGN without passing through late endosomes or the ERC. Each pathway may exist in cells, and the exact route followed would then depend on the transmembrane protein itself.

We described recently the transport of a chimeric transmembrane protein, Tac-TGN38, to the TGN of CHO-derived TRVb-1 cells via the endocytic recycling pathway (Ghosh et al., 1998). This protein is delivered to the TGN by iterative removal from the recycling pathway, recycling multiple times on average before reaching the TGN. Importantly, Tac-TGN38 appears to bypass late endosomes entirely, and we have proposed instead that it is delivered from the recycling compartment itself to the TGN. A very similar trafficking itinerary was reported for the Shiga toxin B-fragment (Mallard et al., 1998). To determine if other membrane proteins use this pathway to reach the TGN from the plasma membrane, we have expressed another chimeric protein, Tac-furin, in TRVb-1 cells. The Tac-furin chimera incorporates the cytoplasmic domain of furin, which comprises the rapid internalization and TGN targeting sequences, with the transmembrane and lumenal domains of the Tac antigen (Bosshart et al., 1994). This architecture allows us to determine the postendocytic transport route of the chimera by detecting internalized anti-Tac antibodies at various stages of transport. We find that, in contrast to Tac-TGN38, Tac-furin does not enter the endocytic recycling pathway. Rather, the protein is delivered to the TGN via late endosomes. Consistent with these two distinct endocytic routes to the TGN, delivery of internalized Tac-furin to the TGN was inhibited by nocodazole, which did not significantly alter Tac-TGN38 transport. Also, Tac-furin accumulated in late endosomes in the presence of wortmannin, whereas Tac-TGN38 was removed slowly from the recycling pathway and delivered to the TGN. Finally, whereas Tac-TGN38 is delivered to the TGN by iterative sorting over multiple passes through the recycling pathway, Tac-furin is transported to the TGN via a single pass through late endosomes. We have therefore characterized two independent pathways from endosomes to the TGN.

Materials and Methods

Cells and Constructs

Chimeric Tac-furin protein constructs TTF and TFF in the plasmid pCDM8.1 incorporating the cytomegalovirus promoter were obtained from Michael Marks (University of Pennsylvania, Philadelphia, PA) (Bosshart et al., 1994), and Juan Bonifacino (National Institutes of Health, Bethesda, MD) (Wolins et al., 1997). TRVb-1 cells are a CHO cell line which lacks endogenous transferrin receptors but stably expresses the human transferrin receptor (McGraw et al., 1987). TRVb-1 cells were cotransfected with the Tac-furin plasmids and the pMEP plasmid (encoding resistance to hygromycin) using the LipofectAMINE reagent system (GIBCO BRL). Cells expressing Tac-furin constructs were selected by culturing in 200 U/ml hygromycin. Clonal populations of the TTF and TFF expressing cells were isolated for quantitative analyses. TRVb-1/Tac-TGN38 cells were described previously (Ghosh et al., 1998). TRVb-1 cells expressing Tac-furin chimeras or Tac-TGN38 were propagated as described previously (Ghosh et al., 1998), except that TRVb-1/Tac-furin cells were grown in the presence of 200 U/ml hygromycin.

Antibodies and Fluorescent Reagents

Monoclonal antibodies (IgG1) against Tac were purified from ascites fluid prepared from the hybridoma cell line 2A3A1H (ATCC) using protein G affinity chromatography. Antibodies were conjugated to Cy3 (Cy3–anti-Tac) (Amersham North America), Alexa 488 (A488–anti-Tac) (Molecular Probes), or fluorescein isothiocyanate (FITC–anti-Tac) (Molecular Probes) according to the manufacturers' instructions. For some experiments, antibodies were labeled with $Na^{125}I$ as described previously (Yamashiro et al., 1984). Low density lipoproteins (LDLs) labeled with DiI were prepared as described (Pitas et al., 1981). Human apotransferrin (Sigma Chemical Co.) was iron-loaded as described previously (Yamashiro et al., 1984) and conjugated to Cy3, Cy5 (Amersham), or Alexa 488 according to the manufacturers' instructions. NBD-C_6-ceramide [N-(ϵ-7-nitrobenz-2-oxa-1,3-diazol-4-yl-aminocaproyl)-D-erythro-sphingosine] and fixable 70-kD dextrans conjugated to rhodamine were purchased from Molecular Probes. Polyclonal antibodies against the cytoplasmic domain of rat TGN38 were obtained from Keith Stanley (Heart Research Institute, Sydney, Australia) (Luzio et al., 1990) or from George Banting (University of Bristol, Bristol, United Kingdom) (Wilde et al., 1992). Polyclonal antibodies against a conserved peptide sequence (TQMNDNRHGTRC) in the furin enzymatic site were obtained from Yukio Ikehara (Fukuoka University, Fukuoka, Japan) (Misumi et al., 1991). Polyclonal antibodies against the CI-MPR were obtained from Peter Lobel (Robert Wood Johnson Medical School, Piscataway, NJ) (Chen et al., 1993). Polyclonal antibodies against fluorescein were purchased from Molecular Probes. Fluorescently labeled polyclonal antibodies against rabbit immunoglobulins were purchased from Sigma Chemical Co., Jackson ImmunoResearch, or Pierce Chemical Co.

Fluorescence Staining Methods

For microscopy, cells were passaged onto poly-D-lysine–treated Number 1 coverslips affixed beneath holes cut into the bottoms of 35-mm Petri dishes. For incubations of live cells with antibodies or ligands, cells were treated as described previously (Ghosh et al., 1998), except as indicated. For indirect immunofluorescence labeling, fixed cells were permeabilized with 0.01% (wt/vol) saponin (Sigma Chemical Co.) in Medium 1 (150 mM NaCl, 20 mM Hepes, 1 mM $CaCl_2$, 5 mM KCl, 1 mM $MgCl_2$, pH 7.4) with 0.5% BSA (AB buffer). Antibodies were diluted into AB buffer for application to cells, and all washes were with AB buffer. Labeling with NBD-C_6-ceramide (Pagano et al., 1989) was performed as described (Ghosh et al., 1998).

Microscopy

Digital epifluorescence microscopy (see Figs. 3, 4 D, and 5, E and F) was performed as described previously (Ghosh et al., 1998). Confocal microscopy was performed using an MRC600 laser scanning unit (BioRad) and an Axiovert 35 microscope (Carl Zeiss) with a 63× 1.4 NA plan Apochromat objective (Zeiss) (see Figs. 4, 6, and 7), or an LSM 510 laser scanning unit (Zeiss) and an Axiovert 100M inverted microscope (Zeiss) with a 63× 1.4 NA plan Apochromat objective (Zeiss) (see Figs. 1, 2, 5, A–D, 8, and 9). Excitation on the MRC600 unit was with a 25-mW argon ion laser emitting at 488 nm and 514 nm, and emissions were collected using standard fluorescein and rhodamine filter sets. Excitation on the LSM 510 unit was with a 25-mW argon laser emitting at 488 nm, a 1.0-mW helium/neon laser emitting at 543 nm, and a 5.0-mW helium/neon laser emitting at 633 nm; emissions were collected using a 505–530-nm band pass filter to collect fluorescein and Alexa 488 emissions and a 585-nm long pass filter to collect rhodamine, Cy3, and DiI emissions. For Fig. 5, Cy3 emissions were collected with a 560–615-nm band pass filter, and Cy5 emissions were collected with a 650-nm long pass filter. Typically, 0.5-μm vertical steps were used, with a vertical optical resolution of <1.0 μm.

Kinetic Experiments

To determine the rate of Tac-furin externalization by accumulation of fluorescent antibodies, TRVb-1/Tac-furin cells cultured on coverslips were incubated with Cy3–anti-Tac IgG (3 μg/ml) in McCoy's 5A + 0.1% BSA for 5, 10, 15, 20, 30, 40, 50, 60, 75, or 90 min. Unbound antibody was removed by washing, and cells were fixed. Cy3 fluorescence was imaged by epifluorescence microscopy. Fluorescence power per cell was determined as described below. Fluorescence power was relatively uniform among all cells for each time point.

Determination of the externalization rate by accumulation of radiolabeled antibodies, measurement of the level of surface expression of Tac-furin, and determination of the endocytic rate constant of Tac-furin (Wiley and Cunningham, 1982) were performed using procedures described previously (Ghosh et al., 1998).

To determine the exit rate of antibody-labeled Tac-furin from the cell, TRVb-1/Tac-furin cells were incubated with FITC–anti-Tac for 60 min, followed by a 30-min chase in McCoy's/BSA. After this procedure, anti-Tac is mostly detected in the TGN (see Fig. 3 D). Cells were further incubated for 5, 10, 15, 20, 30, 40, 50, 60, 75, or 90 min in the presence of antifluorescein antibodies (10 μg/ml) in the chase medium and fixed. We have shown previously that antifluorescein antibodies are not internalized by fluid-phase pinocytosis sufficiently to cause significant intracellular quenching (Ghosh et al., 1998). Fluorescein fluorescence was imaged by epifluorescence microscopy. Fluorescence power per cell was determined as described below. Cells that did not receive antifluorescein exhibited insignificant loss of fluorescence over the chase period (data not shown). To determine if Tac-furin undergoes rapid endocytic recycling, TRVb-1/Tac-furin cells were incubated with FITC-anti-Tac for 10 min, then washed in medium and chased in the absence or presence of antifluorescein for 5, 10, 15, or 20 min. Cells were fixed, and fluorescein fluorescence was imaged as described above.

Nocodazole and Wortmannin Studies

Experiments examining the effects of nocodazole and wortmannin on protein transport were performed in parallel. For all steps, BSA was omitted from incubation media to prevent adsorption and deactivation of reagents, and all cells received 0.1% (vol/vol) DMSO to control for effects of the solvent. Nocodazole-treated cells were pretreated with nocodazole (33 μM) for 30 min at 4°C, then 30 min at 37°C. To maintain identical conditions of temperature and DMSO exposure, wortmannin-treated cells were incubated for 30 min at 4°C in the presence of 0.1% DMSO, then pretreated with wortmannin (100 nM) for 30 min at 37°C. Untreated cells were incubated for 30 min at 4°C and 30 min at 37°C in the presence of 0.1% DMSO. After pretreatments, cells were incubated with ligands for 15 min followed by a 45-min chase in the continuous presence of nocodazole, wortmannin, or DMSO alone, respectively.

Image Processing and Quantification

Processing of digitized images was performed using the MetaMorph image processing software package (Universal Imaging). All images were corrected for background fluorescence and crossover between channels. To quantify fluorescence power per cell (see Figs. 3, A and C, and 4 D), the background fluorescence value was subtracted from images, and the remaining fluorescence power in the field was summed and divided by the number of cells in the field; typically, 10 fields of ~20 cells per field were analyzed for each data point in a single experiment. For quantitative microscopic analyses and ^{125}I-antibody experiments, data points were fit using the SigmaPlot software program (SPSS Inc.).

To quantify the colocalization of internalized fluorescent anti-Tac and LDL over a time course, cells were imaged using the MRC600 confocal microscope. Using routines available in the MetaMorph software package, images from the green and red channels were thresholded to detect labeled objects above background fluorescence, then labeled endosomes were selected on the basis of size (between 10 and 50 square pixels). Double-labeled endosomes were identified by performing a logical AND operation with the endosomes detected in the green and red channels. Intensities of singly and doubly labeled endosomes were transferred to Microsoft Excel for statistical analyses.

Results

Internalized Tac-Furin Is Delivered to the TGN

Tac-furin (TTF) was shown by Bonifacino and co-workers to cycle between the plasma membrane and the TGN, maintaining a steady-state enrichment in the TGN (Bosshart et al., 1994); similar behavior of exogenously expressed epitope-tagged furin was described by Thomas and co-workers (Molloy et al., 1994). We transfected TRVb-1 cells with the TTF form of Tac-furin and isolated clonal populations expressing the chimeric construct (referred to as TRVb-1/TTF cells). Results presented here were indistinguishable from those observed for two different clones and for a polyclonal population; images and data from a single clone are presented. At steady state, we observed Tac-furin predominantly in the TGN, where it colocalized with endogenous furin and with TGN38 (Fig. 1, A and B). The immunolocalized Tac-furin was not seen in endosomes labeled with antibodies to the CI-MPR (Fig. 1 C) or with internalized dextrans (Fig. 1 D), indicating that the expressed chimera is not detectable in endosomes at steady state. We observed that the overlap of Tac-furin and endogenous furin was incomplete (Fig. 1 A). This may be due to the transport of a portion of endogenous furin into the degradative pathway (Wolins et al., 1997). Alternatively, the two molecules may be partially distributed into distinct subdomains of the TGN (Berger et al., 1995; Ladinsky et al., 1999).

When TRVb-1/TTF cells were incubated with fluorescently labeled anti-Tac antibodies, the antibodies were internalized and transported over time to the TGN, which was identified using anti-TGN38 antibodies (Fig. 2), using antibodies against furin, or using the fluorescent lipid analogue NBD-C_6-ceramide (data not shown). Tac-furin was detected in the TGN after ~30 min of internalization (Fig. 2, E and F), becoming further enriched there after 60 min (Fig. 2, G and H). These results demonstrate the transport of Tac-furin to the TGN in our system and confirm previous reports in other cell types. Internalized anti-Tac Fab fragments were transported identically to intact IgG (data not shown), demonstrating that our findings are not an artifact of protein aggregation by divalent IgG. The delivery of internalized anti-Tac to the TGN in TRVb-1/TTF cells allowed us to describe the kinetics of Tac-furin trafficking by incubating cells with anti-Tac under various conditions.

Kinetic Parameters of Tac-Furin Transport

To determine the rate of exit of Tac-furin from TRVb-1/TTF cells, the cells were incubated at 37°C with Cy3–anti-Tac, and the cells were imaged by epifluorescence microscopy. The accumulation of the Cy3–anti-Tac was then quantified in terms of fluorescence power per cell versus incubation time (Fig. 3 A, solid line). Under these conditions, the rate of accumulation of anti-Tac is equal to the rate of appearance of unlabeled intracellular Tac-furin at the plasma membrane (Ghosh et al., 1995). We found that the antibody was accumulated by TRVb-1/TTF cells with first-order kinetics, with a half-time of ~26 min (k = 0.026 min^{-1}).

Alternatively, cells in a 24-well plate were incubated at 37°C for various times with ^{125}I–anti-Tac antibodies, and

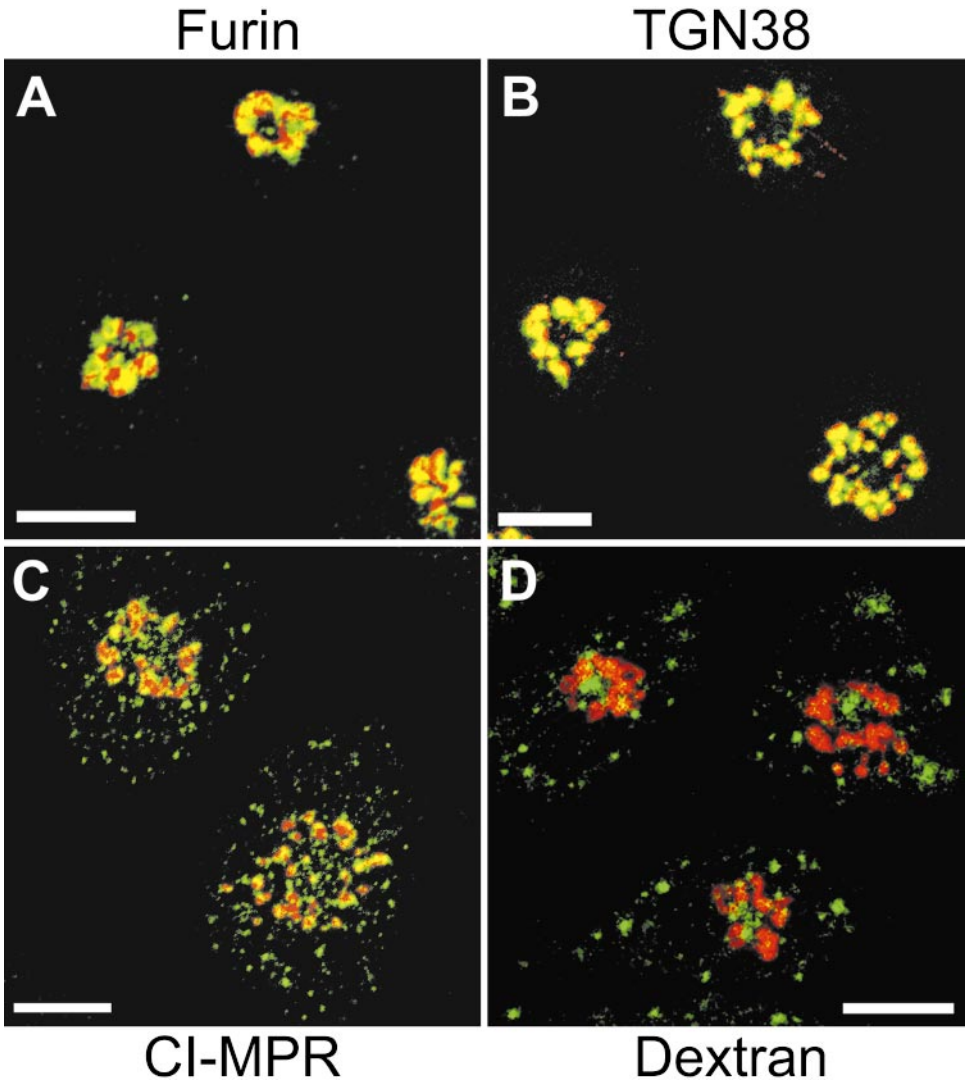

Figure 1. Recombinantly expressed Tac-furin localizes to the TGN at steady state. TRVb-1/TTF cells were fixed in 4% paraformaldehyde and permeabilized with 0.01% saponin in Medium 1 with 0.5% (wt/vol) BSA. Cells were incubated with Cy3–anti-Tac (red) and polyclonal antibodies against furin (green, A), TGN38 (green, B), or CI-MPR (green, C) followed by Alexa 488 goat anti–rabbit secondary antibodies. In D, cells were incubated with fluorescein-conjugated dextrans (green) for 1 h before fixation, permeabilization, and staining with Cy3–anti-Tac (red). Z-series confocal projections are shown. Pixels labeled with both fluorophores appear yellow. Bars, 10 μm.

the cell-associated radioactivity was measured for each time point. We found that the cells accumulated anti-Tac with a half-time of ~36 min (k = 0.019 min^{-1}) (Fig. 3 A, dashed line). The difference in the exit rate constants obtained from the two different methods is small compared with other parameters of Tac-furin trafficking (see below), and may be due to the differences in the experimental procedures. From the specific activity of the ^{125}I–anti-Tac, the asymptote of the accumulation curve, and the number of cells in each well, we calculate that ~2×10^5 copies of Tac-furin are expressed per cell. Tac-furin and endogenous furin localize predominantly to the TGN in these cells (Fig. 1 and data not shown), so it is unlikely that sorting or retention mechanisms are saturated at this expression level.

To determine the steady-state surface expression of Tac-furin, TRVb-1/TTF cells were incubated with ^{125}I–anti-Tac antibody at 0°C to prevent internalization, and the bound counts were compared with the asymptote of the 37°C ^{125}I–anti-Tac accumulation curve. We estimate that 5% of Tac-furin is at the plasma membrane at steady state (data not shown).

We also measured the internalization rate constant of Tac-furin in TRVb-1/TTF cells. As determined from the ratios of internal to surface antibody over a brief time course at 37°C, the protein is internalized with a rate constant of 0.36 min^{-1}, which is consistent with the presence of rapid internalization signals in the furin cytoplasmic domain (Fig. 3 B). At steady state, the relative rates of internalization and externalization determine the relative amounts of protein in internal compartments and at the plasma membrane. The ratio of the measured rates of endocytosis (0.36 min^{-1}) and externalization (0.019 min^{-1}) of ^{125}I–anti-Tac is about 19, which agrees well with the estimated internal-to-surface ratio of Tac-furin (also about 19). This indicates that our kinetic data accurately describe the rates of trafficking of Tac-furin.

To demonstrate that antibody labeling did not perturb the kinetics of Tac-furin trafficking, we measured the externalization rate by another method. TRVb-1/TTF cells were incubated for 60 min with FITC–anti-Tac, followed by a 30-min chase. At this time, the FITC–anti-Tac predominantly labeled the TGN (Fig. 3 D). Subsequently, antifluorescein was applied to the medium, and the cells were incubated over a long time course to allow external-

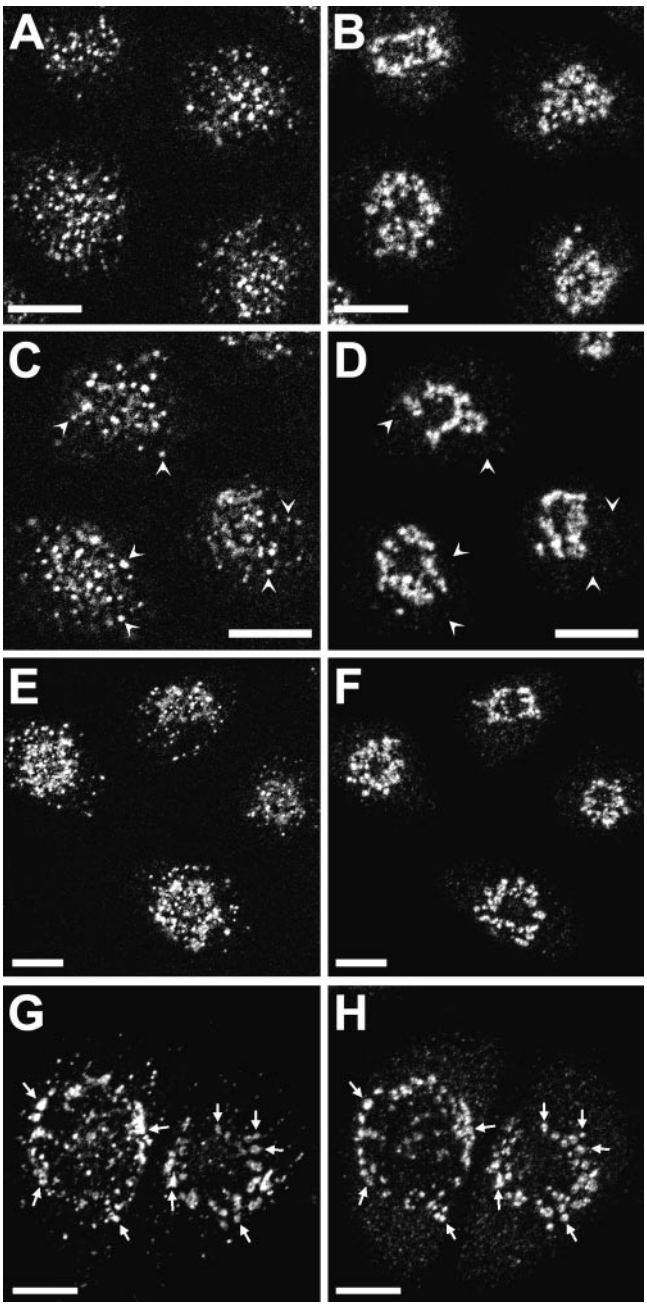

Figure 2. Accumulation of internalized Tac-furin in the TGN. TRVb-1/TTF cells were incubated with Cy3–anti-Tac antibody for 10 (A), 20 (C), 30 (E), or 60 min (G). Cells were fixed, permeabilized, and stained with anti-TGN38 polyclonal antibodies and Alexa 488 goat anti–rabbit secondary antibodies (B, D, F, and H). Z-series confocal projections are shown. Arrowheads in C and D point to endosomes containing Tac-furin but not TGN38. Arrows in G and H point to TGN elements labeled with both probes. Bars, 10 μm.

ization of Tac-furin. Over this time period, the pericentriolar fluorescence signal decreased, indicating that the antibody was externalized from the TGN to the plasma membrane (Fig. 3 E). Cells were then imaged by epifluorescence microscopy, and the fluorescein fluorescence power per cell was quantified for each time point (Fig. 3 C). The fluorescence power declined in a monoexponential fashion ($k = 0.026\ min^{-1}$), with a half-time of about 26 min indicating the rate of exit of FITC–anti-Tac–labeled Tac-furin from the cells. This rate is similar to the rate of externalization of unlabeled Tac-furin from cells (Fig. 3 A), confirming that antibody labeling has not altered the kinetics of Tac-furin transport. Since the majority of the FITC–anti-Tac was externalized from the TGN under this procedure, the measured rate constant mainly reflects the rate of transport of Tac-furin from the TGN to the plasma membrane. The exact pathway and the rate of exit of Tac-furin from the TGN per se are not directly shown by these studies.

The agreement of this rate constant with that for whole-cell antibody accumulation is consistent with the existence of a single major exit route for Tac-furin (see below). Also, the fluorescein quenching procedure measures only the kinetics of externalization of the cycling Tac-furin pool. Our results suggest either that the cycling and biosynthetic pools are externalized at the same rate or that the contribution of the biosynthetic pool to these kinetics is small. Finally, the transport of FITC–anti-Tac back to the plasma membrane demonstrates that the antibody remains associated with Tac-furin throughout its trafficking itinerary. Otherwise, dissociated FITC–anti-Tac would accumulate in lysosomes, which was not observed. The low level of residual fluorescence power observed in these experiments after a prolonged chase is probably due to autofluorescence and the incomplete quenching of fluorescein by antifluorescein antibodies, as little TGN or endosomal anti-Tac staining could be detected at the longest time points. The rapid internalization of Tac-furin at the plasma membrane and the relatively slow movement from the TGN to the plasma membrane account for the steady-state localization of the chimera.

Tac-Furin Is Delivered to the TGN via Late Endosomes

We next determined the route by which Tac-furin is transported to the TGN. To evaluate if Tac-furin, like Tac-TGN38, transits through the endocytic recycling pathway, TRVb-1/TTF cells were incubated for 5 min with fluorescently-labeled anti-Tac and transferrin, then fixed immediately or chased in the continuous presence of transferrin to label the recycling pathway (Fig. 4, A–C). As reported previously (Hopkins and Trowbridge, 1983; Yamashiro et al., 1984), transferrin was detected primarily in the pericentriolar ERC and also in peripheral sorting endosomes. In contrast, Tac-furin was observed in an exclusively punctate distribution at early chase times (Fig. 4, A and B), accumulating in the TGN after a 40-min chase (Fig. 4 C). In the absence of a chase, the two molecules partially colocalized in sorting endosomes (data not shown), and the extent of colocalization declined rapidly with increasing chase times. At no time was Tac-furin prominent in the ERC, unlike Tac-TGN38 which is enriched in that organelle shortly after internalization (Ghosh et al., 1998).

We also found that endocytosed Tac-furin does not recycle rapidly to the plasma membrane. TRVb-1/TTF cells were incubated briefly with anti-Tac conjugated to fluorescein (FITC–anti-Tac), then chased over a short time course in the absence or presence of antifluorescein anti-

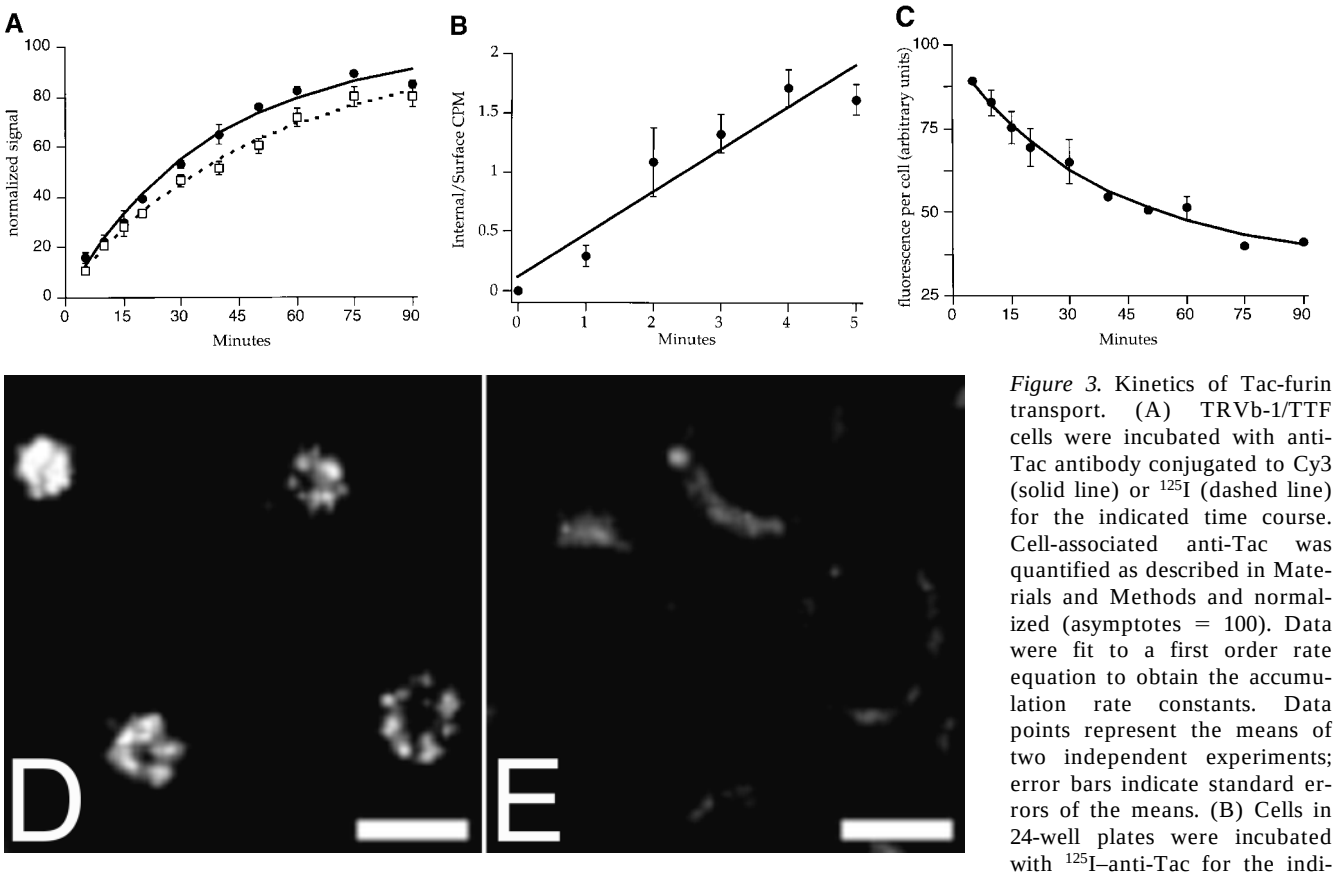

Figure 3. Kinetics of Tac-furin transport. (A) TRVb-1/TTF cells were incubated with anti-Tac antibody conjugated to Cy3 (solid line) or ^{125}I (dashed line) for the indicated time course. Cell-associated anti-Tac was quantified as described in Materials and Methods and normalized (asymptotes = 100). Data were fit to a first order rate equation to obtain the accumulation rate constants. Data points represent the means of two independent experiments; error bars indicate standard errors of the means. (B) Cells in 24-well plates were incubated with ^{125}I–anti-Tac for the indicated times at 37°C, then were rapidly shifted to 0°C. Specific internal and surface-bound counts were determined, the ratios were obtained for each sample, and the ratios were averaged among three wells each in four independent experiments. Means ± SEM are plotted. Data were fitted to a straight line to obtain the internalization rate constant for Tac-furin. (C) Cells were incubated with FITC–anti-Tac to allow the antibody to accumulate in the TGN, then were incubated in the presence of antifluorescein antibodies for the indicated times. Cell-associated fluorescence was calculated per cell as described in Materials and Methods. Means ± SEM are plotted for two independent experiments. Data were fitted to a monoexponential decay to obtain the externalization rate constant. (D) Representative field of cells labeled with fluorescein–anti-Tac as described in C and chased for 10 min in the presence of antifluorescein antibodies. (E) Representative field after a 90-min chase in the presence of antifluorescein antibodies. The dim, hazy fluorescence is at the borders of the cells, and is not in a pattern resembling the TGN. Epifluorescence micrographs are shown. Bars, 10 μm.

bodies in the medium. Cells were imaged by epifluorescence microscopy, and the fluorescence power per cell was determined for each chase time point (Fig. 4 D). If Tac-furin is rapidly recycled, then the internalized FITC–anti-Tac should reappear at the plasma membrane, where its fluorescence would be quenched by the antifluorescein antibodies. Instead, we observed no loss of cell-associated fluorescence over the time of the chase. This finding again contrasts with the rapid recycling of the bulk of internalized Tac-TGN38, which was demonstrated using the same approach (Ghosh et al., 1998).

The most common fate of an endocytosed protein that is not recycled is accumulation in endosomes that over time have matured and are segregated from the recycling pathway. This class of endosomes is defined as late endosomes (Dunn and Maxfield, 1992). For example, internalized LDL dissociates from its receptor in sorting endosomes and then is transported to late endosomes (Goldstein et al., 1985; Dunn et al., 1989), where it no longer colocalizes with internalized transferrin. Also, growth factor receptors such as the epidermal growth factor receptor are transported to late endosomes and lysosomes after binding to their corresponding ligands (Dunn et al., 1986; Miller et al., 1986; Jackle et al., 1991). A population of late endosomes is enriched in the CI-MPR (Willingham et al., 1983; Geuze et al., 1984; Griffiths et al., 1988). To begin to characterize the endosomal intermediate in Tac-furin trafficking, we incubated TRVb-1/TTF cells for 5 min with anti-Tac antibody and chased for various times. Fluorescent transferrin was applied during the last 5 min of the chase to label sorting endosomes and the ERC. After fixation, the cells were permeabilized and stained for the CI-MPR by indirect immunofluorescence (Fig. 5). At all time points, anti-Tac exhibited a detectable but low degree of colocalization with the CI-MPR (Fig. 5, A and B, and data not shown). In the absence of chase, internalized anti-Tac colocalized with transferrin in punctate sorting endosomes (data not shown). This colocalization was lost with a chase, as anti-Tac distributed into endosomes near the center of the cell at 20 min (Fig. 5 C) and then eventually accumulated in the TGN at 40 min (Fig. 5 D). Since the anti-Tac–labeled endosomes observed at 20 min of chase do not contain

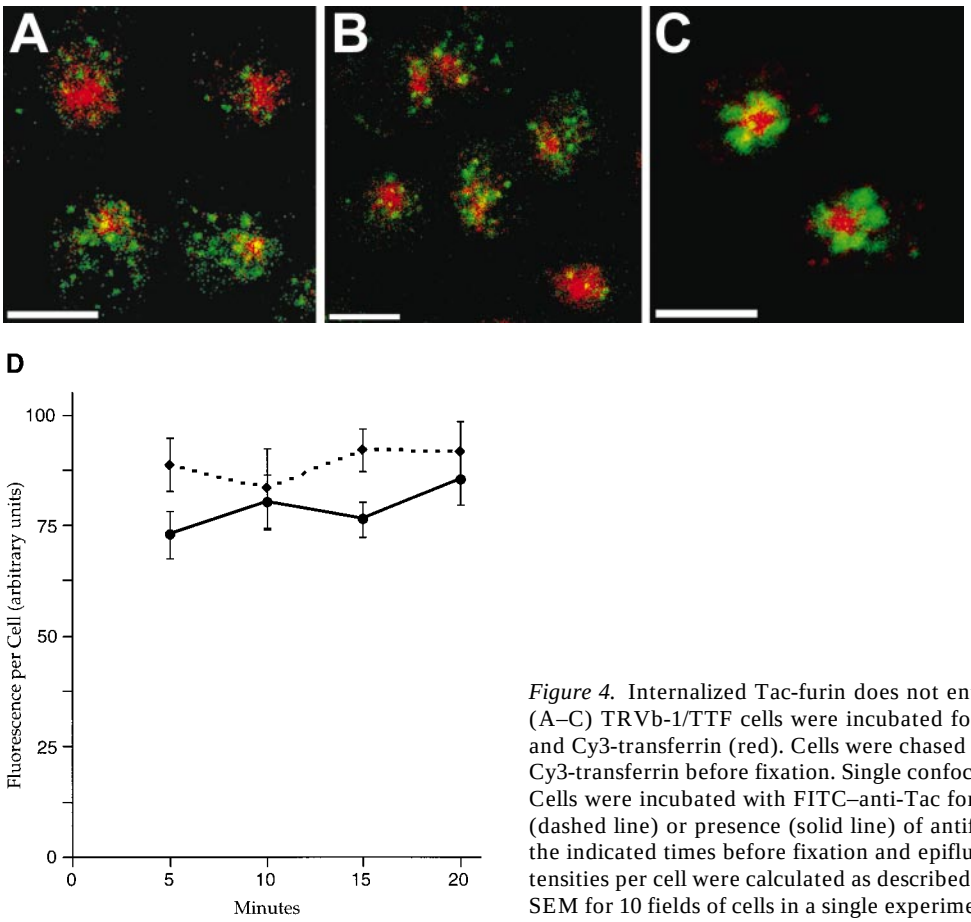

Figure 4. Internalized Tac-furin does not enter the endocytic recycling pathway. (A–C) TRVb-1/TTF cells were incubated for 5 min with FITC–anti-Tac (green) and Cy3-transferrin (red). Cells were chased for 5 (A), 10 (B), or 40 min (C) with Cy3-transferrin before fixation. Single confocal slices are shown. Bars, 10 μm. (D) Cells were incubated with FITC–anti-Tac for 10 min, then chased in the absence (dashed line) or presence (solid line) of antifluorescein polyclonal antibodies for the indicated times before fixation and epifluorescence imaging. Fluorescence intensities per cell were calculated as described in Materials and Methods. Means ± SEM for 10 fields of cells in a single experiment are shown.

transferrin, they are presumably matured endosomes that have departed the recycling pathway.

The absence of Tac-furin from CI-MPR–enriched endosomes may be due to transport into a novel pathway distinct from the classical degradative pathway, or may be explained by the exit of Tac-furin from endosomes before they have become significantly enriched in CI-MPR. The existence of multiple classes of matured endosomes with distinct properties has been reported in other systems (Aniento et al., 1993; Gruenberg and Maxfield, 1995; Kleijmeer et al., 1997). To establish the point at which a molecule that follows the degradative pathway colocalizes with the CI-MPR, fluorescent dextrans were followed through a pulse-chase protocol over the same time course. The dextrans were not enriched in CI-MPR–positive endosomes until 40 min of chase (Fig. 5, E and F), at which time anti-Tac had already accumulated in the TGN. Therefore, transport of lysosomally targeted cargo into CI-MPR–containing endosomes may occur after the time of endosome maturation. This would allow a molecule such as Tac-furin to enter newly formed late endosomes and then exit before extensive delivery of the CI-MPR into this compartment.

To confirm that endocytosed Tac-furin enters late endosomes, TRVb-1/TTF cells were pulsed for 5 min with fluorescently labeled anti-Tac and LDL (Fig. 6). After a 5-min chase, the two probes were detected in peripheral spots, colocalizing significantly although incompletely (Fig. 6 A). The frequency of double-labeled endosomes remained high through about 15–20 min of chase (Fig. 6 B, yellow spots). At these chase times, the majority of LDL is in late endosomes (Salzman and Maxfield, 1989; Dunn and Maxfield, 1992), segregated from recycling molecules such as transferrin. Therefore, the colocalization of anti-Tac with LDL demonstrates the transport of Tac-furin into late endosomes. After a longer chase interval (Fig. 6 D), anti-Tac no longer colocalized with LDL and was instead found in a compartment resembling the TGN. When anti-Tac and LDL were applied to cells with consecutive pulses, such that one probe experienced a 20-min chase and the other was not allowed a chase, the two probes did not colocalize (data not shown). This result indicates that the overlap of anti-Tac and LDL illustrated in Fig. 6 is not in sorting endosomes that have not yet matured. Also, anti-Tac rapidly lost colocalization with transferrin-containing peripheral punctate sorting endosomes over this time course (Figs. 4 and 5). Transport of internalized Tac-furin through late endosomes en route to the TGN was also demonstrated by colocalization in punctate structures with internalized dextrans over a similar time course (data not shown).

The extent of colocalization of anti-Tac and LDL was quantified by two different computational methods. Endosomes labeled with LDL were selected, and the proportion

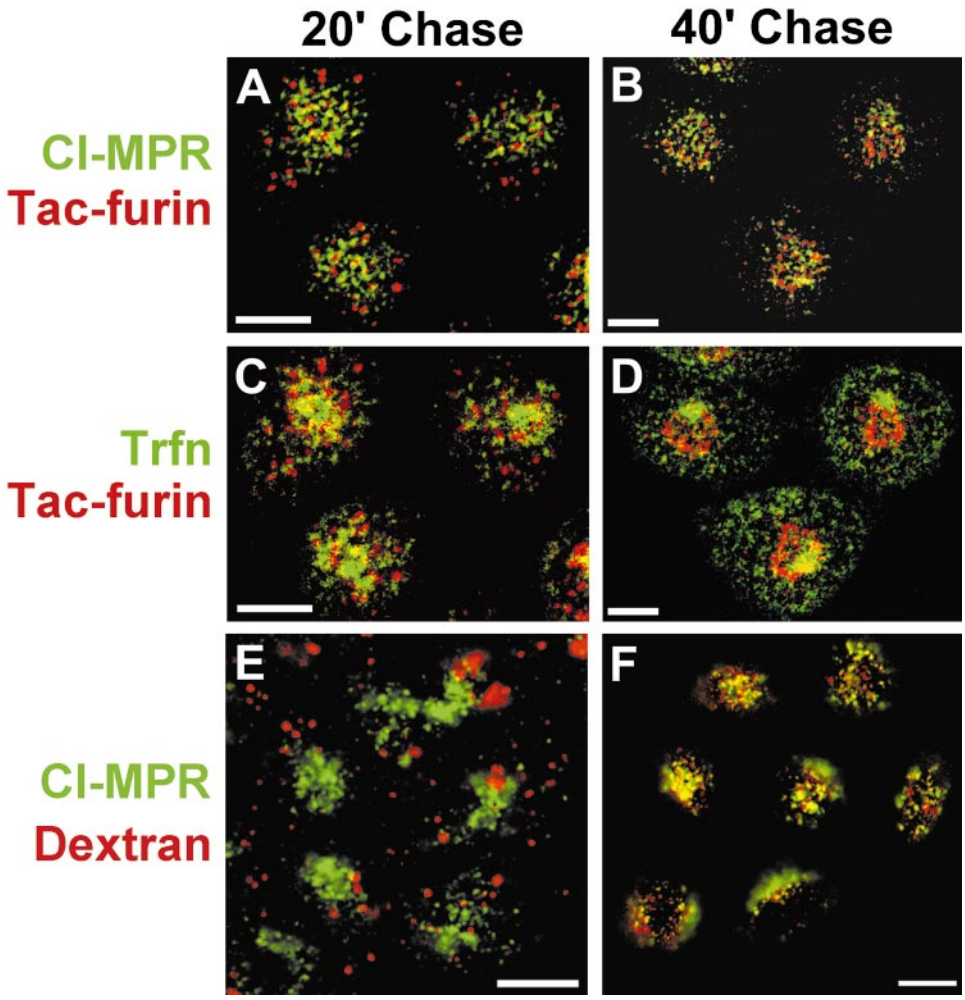

Figure 5. Internalized Tac-furin is delivered to the TGN without accumulation into CI-MPR–labeled endosomes. (A–D) TRVb-1/TTF cells were incubated with Cy3–anti-Tac (red) for 5 min and chased for 20 or 40 min as indicated. Cy5-transferrin (Trfn, green in C and D) was present for the last 5 min of the chase. Cells were fixed, permeabilized, and labeled with polyclonal antibodies against CI-MPR followed by Alexa 488 goat anti–rabbit secondary antibodies (green in A and B). (E and F) TRVb-1 cells were incubated with rhodamine-dextrans (red) for 5 min and chased for 20 or 40 min as indicated. Cells were stained for CI-MPR (green) as in A–D. Z-series confocal projections (A–D) and epifluorescence micrographs (E and F) are shown. Pixels labeled with both fluorophores appear yellow. Bars, 10 μm.

that was also labeled with anti-Tac was quantified versus chase time. Also, the ratio of anti-Tac to LDL fluorescence was measured for each double-labeled endosome, and the distribution of these ratios was determined as a function of chase time. These analyses were performed on images similar to those in Fig. 6, using two independent data sets. We found that the proportion of LDL-labeled endosomes containing anti-Tac declined sharply between 20 and 40 min of chase, coincident with the appearance of anti-Tac in the TGN (Fig. 7 A). In contrast, the population of endosomes labeled with both probes exhibited no change in fluorescence power ratios during this same interval (Fig. 7 B), although the size of that population decreased over time. The abrupt loss of double-labeled endosomes and the relative invariance of fluorescence power ratios suggest that anti-Tac may be sorted away from LDL by a highly concerted process, rather than by a more gradual or iterative mechanism; in this way, a double-labeled endosome would suddenly become singly labeled. We failed to detect an accumulation of endosomes labeled with anti-Tac and not with LDL, so it seems plausible that Tac-furin follows a relatively direct route from endosomes to the TGN. This event apparently precedes or coincides with the delivery of CI-MPR to late endosomes from the TGN, such that the two molecules mostly do not overlap.

The Transmembrane Domain of Furin Does Not Encode Essential Endosomal Sorting Information

In addition to cytoplasmic domain sorting signals, the transmembrane domains of some membrane proteins have been shown to perform a sorting function. In particular, the transmembrane domain of TGN38 has been shown to play a role in the localization of that protein to the TGN (Ponnambalam et al., 1994). To determine if the transmembrane domain of furin influences its postendocytic trafficking, we expressed in TRVb-1 cells a construct encoding the ectodomain of Tac and the transmembrane and cytoplasmic domains of furin (TFF) (Wolins et al., 1997). We found that this chimeric protein, like TTF, was internalized and entered late endosomes, bypassing the recycling pathway (data not shown). The internalized chimeras entered the TGN over a similar time course, and the rates of externalization from cells were almost identical for each protein (k_e = 0.023 min^{-1} for TFF, and 0.025 min^{-1} for TTF in a single experiment). Therefore, the transmembrane domain appears not to be a major sorting determinant of the endocytic transport of furin to the TGN. The result is consistent with previous findings in other systems (Bosshart et al., 1994; Wolins et al., 1997).

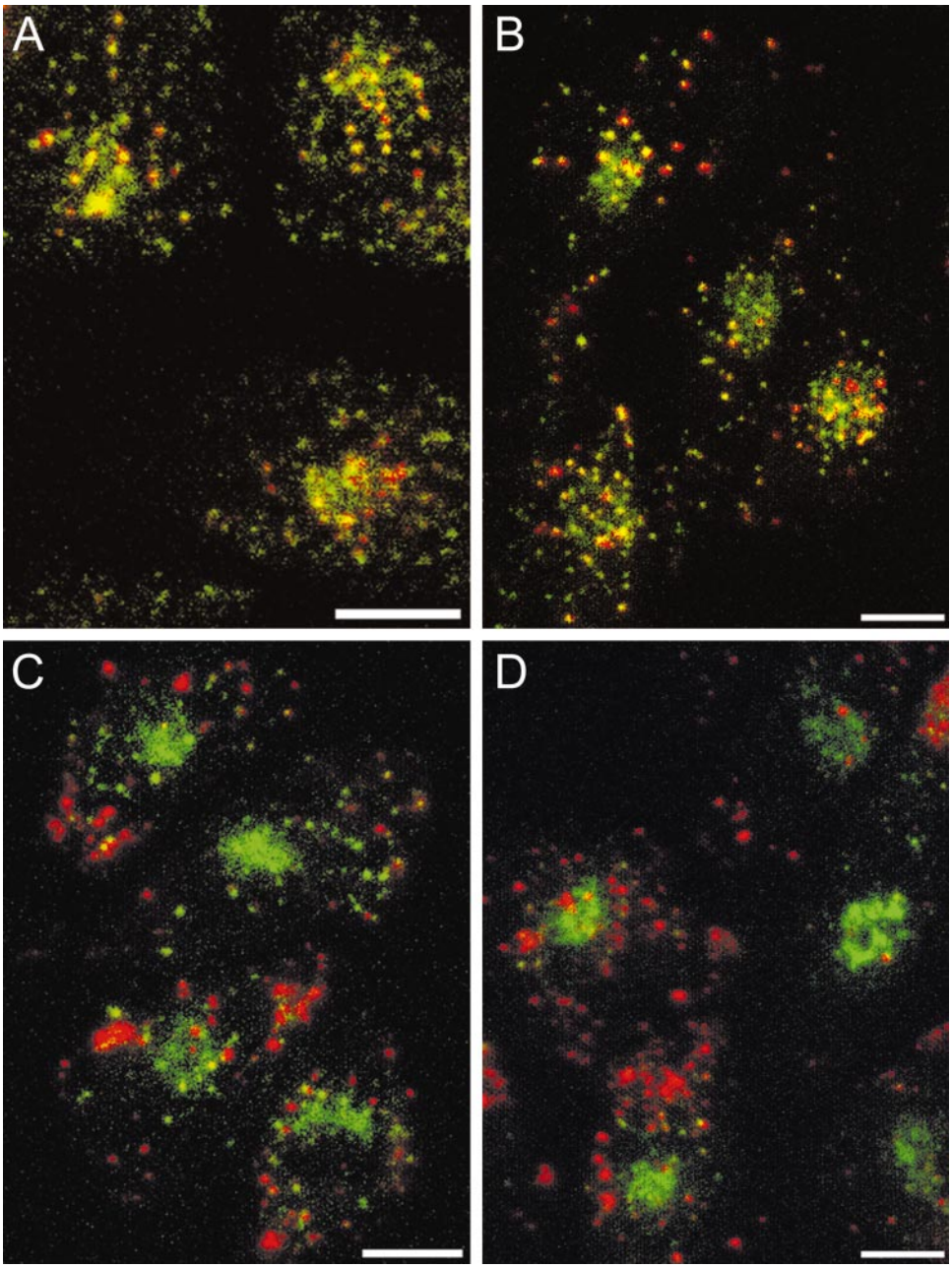

Figure 6. Internalized Tac-furin colocalizes with LDL in sorting and then late endosomes en route to the TGN. TRVb-1/TTF cells were incubated for 5 min with A488–anti-Tac (green) and DiI-LDL (red), then chased for 5 (A), 15 (B), 30 (C), or 40 min (D). Cells were fixed and imaged by confocal microscopy. Z-series confocal projections are shown. Pixels labeled with both fluorophores appear yellow. Bars, 10 μm.

Transport Pathways of Tac-Furin and Tac-TGN38 to the TGN Are Differentially Sensitive to Nocodazole and Wortmannin

The transport of Tac-furin to the TGN via late endosomes is distinct from the pathway that is followed by Tac-TGN38. The point at which the trafficking of the two proteins diverges is the sorting endosome: Tac-furin is retained as the sorting endosome matures into a late endosome, whereas Tac-TGN38 is transported to the ERC. To show directly the divergent routes taken by these two chimeras, we performed a series of pulse-chase experiments under conditions that are known to selectively alter different properties of the endosomal system.

First, we took advantage of the effects of the microtubule-disrupting compound, nocodazole. Nocodazole has been shown to inhibit endosome maturation (Gruenberg et al., 1989; Bomsel et al., 1990) but does not affect the kinetics of internalization or endocytic recycling (Sakai et al., 1991; Takeuchi et al., 1992; Jin and Snider, 1993; McGraw et al., 1993). We verified these effects in TRVb-1 cells expressing Tac-furin (TTF) or Tac-TGN38 (data not shown). Therefore, treatment of cells with nocodazole provides a means to discriminate between transport to the TGN via late endosomes and transport via the recycling pathway. TRVb-1/Tac-TGN38 and TRVb-1/TTF cells were pretreated with 33 μM nocodazole or 0.1% DMSO alone as described in Materials and Methods. The cells were then incubated with fluorescently labeled anti-Tac antibodies, alone or in combination with fluorescent LDL for 15 min, followed by a 45-min chase; nocodazole or DMSO was

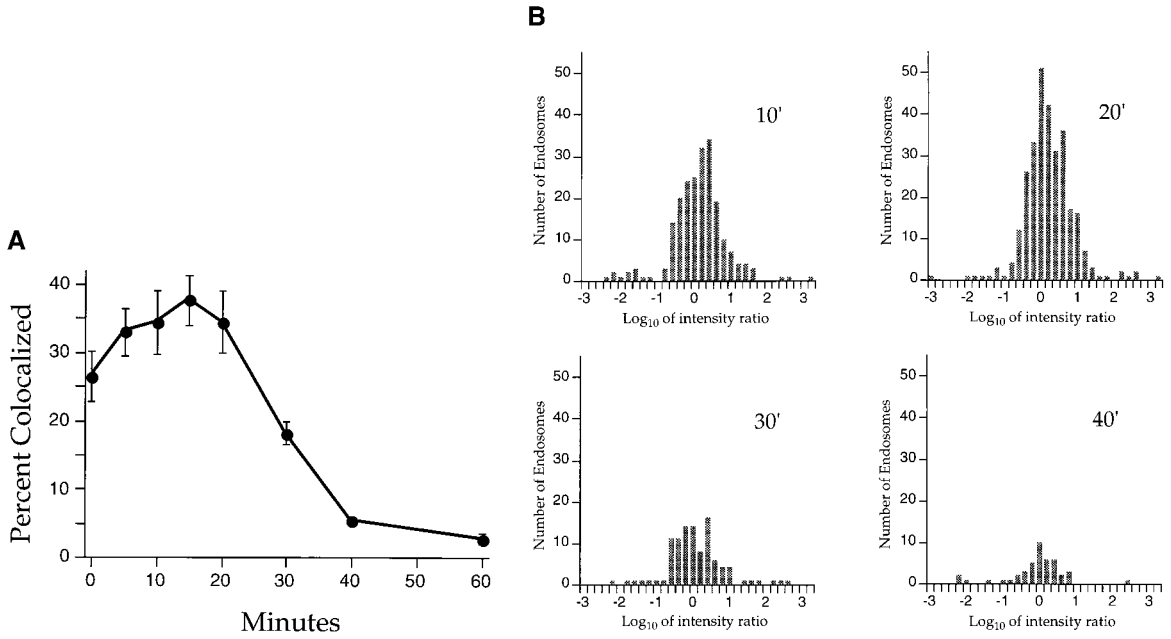

Figure 7. Internalized Tac-furin abruptly exits LDL-labeled endosomes and is delivered to the TGN. Cells were incubated with A488–anti-Tac and DiI-LDL as described for Fig. 5. (A) Endosomes labeled with LDL were selected. The proportion of those endosomes that also labeled with anti-Tac was calculated for five fields for each time point. Data are plotted as mean percent colocalized ± SEM. (B) Endosomes labeled with both LDL and anti-Tac were identified, and the ratio of anti-Tac and LDL fluorescence powers was calculated for each endosome. The common log of each ratio was calculated, and the population of ratios is plotted as a histogram for each time point. The 10-, 20-, 30-, and 40-min histograms are shown. The Kruskal-Wallis analysis of variants indicates that these distributions are not statistically different ($P > 0.1$).

present throughout this time course. After fixation, cells that received anti-Tac alone were stained with NBD-C_6-ceramide to label the TGN. The distributions of the probes were determined by confocal microscopy.

In TRVb-1/TTF cells treated with DMSO alone, internalized antibody colocalized well with NBD-C_6-ceramide (Fig. 8 A) and had very little overlap with LDL, which is expected to label mainly late endosomes after this time course (Fig. 8 B). However, nocodazole treatment resulted in a substantial redistribution of anti-Tac into LDL-containing structures, and overlap with NBD-C_6-ceramide was greatly diminished (Fig. 8, C and D). Note the dispersion of the NBD-C_6-ceramide staining, which is a consequence of the fragmentation of the TGN caused by microtubule disassembly (Rogalski and Singer, 1984; Ladinsky and Howell, 1992). Since nocodazole inhibits endosome maturation, we presume that anti-Tac and LDL label sorting endosomes under these conditions. In contrast, treatment of TRVb-1/Tac-TGN38 cells with nocodazole had little effect on the transport of internalized anti-Tac antibody to the TGN (Fig. 8 E), and the antibody exhibited limited overlap with internalized LDL (Fig. 8 F). These results support the proposal that Tac-furin is directed to the TGN by way of late endosomes, whereas Tac-TGN38 travels via the endocytic recycling pathway.

A second reagent having relevant effects on vesicular transport is the phosphatidylinositol 3-OH kinase (PI3 kinase) inhibitor wortmannin. Wortmannin exerts numerous effects on endosomal trafficking, including the inhibition of early endosome fusion (Jones and Clague, 1995; Li et al., 1995; Spiro et al., 1996), the swelling of late endosomes and impaired transport of hydrolases to lysosomes from the TGN (Brown et al., 1995; Davidson, 1995), acceleration of the rate of transferrin internalization (Martys et al., 1996; Spiro et al., 1996), and a moderate slowing of endocytic recycling (Martys et al., 1996; Shpetner et al., 1996; Spiro et al., 1996). However, wortmannin allows the delivery of internalized material to late endosomes (Martys et al., 1996; Shpetner et al., 1996). These effects were also observed in TRVb-1 cells expressing Tac-furin or Tac-TGN38 (data not shown). Given these findings, we evaluated whether or not wortmannin would affect the transport of Tac-TGN38 or Tac-furin to the TGN from the plasma membrane. TRVb-1/Tac-TGN38 and TRVb-1/TTF cells were pretreated with 100 nM wortmannin or 0.1% DMSO alone as described in Materials and Methods. The cells were then incubated with fluorescently labeled anti-Tac antibodies, alone or in combination with fluorescent LDL for 15 min, then chased for 45 min in the presence or absence of wortmannin. After fixation, cells that received anti-Tac alone were stained with NBD-C_6-ceramide to label the TGN. Samples that were not subjected to a chase were also analyzed to verify the efficient internalization of the probes irrespective of wortmannin treatment (data not shown).

After 45-min chase, anti-Tac mostly labeled the TGN in mock-treated cells, as observed previously (data not shown). The trafficking of Tac-furin was severely inhibited by wortmannin treatment. Under these conditions, inter-

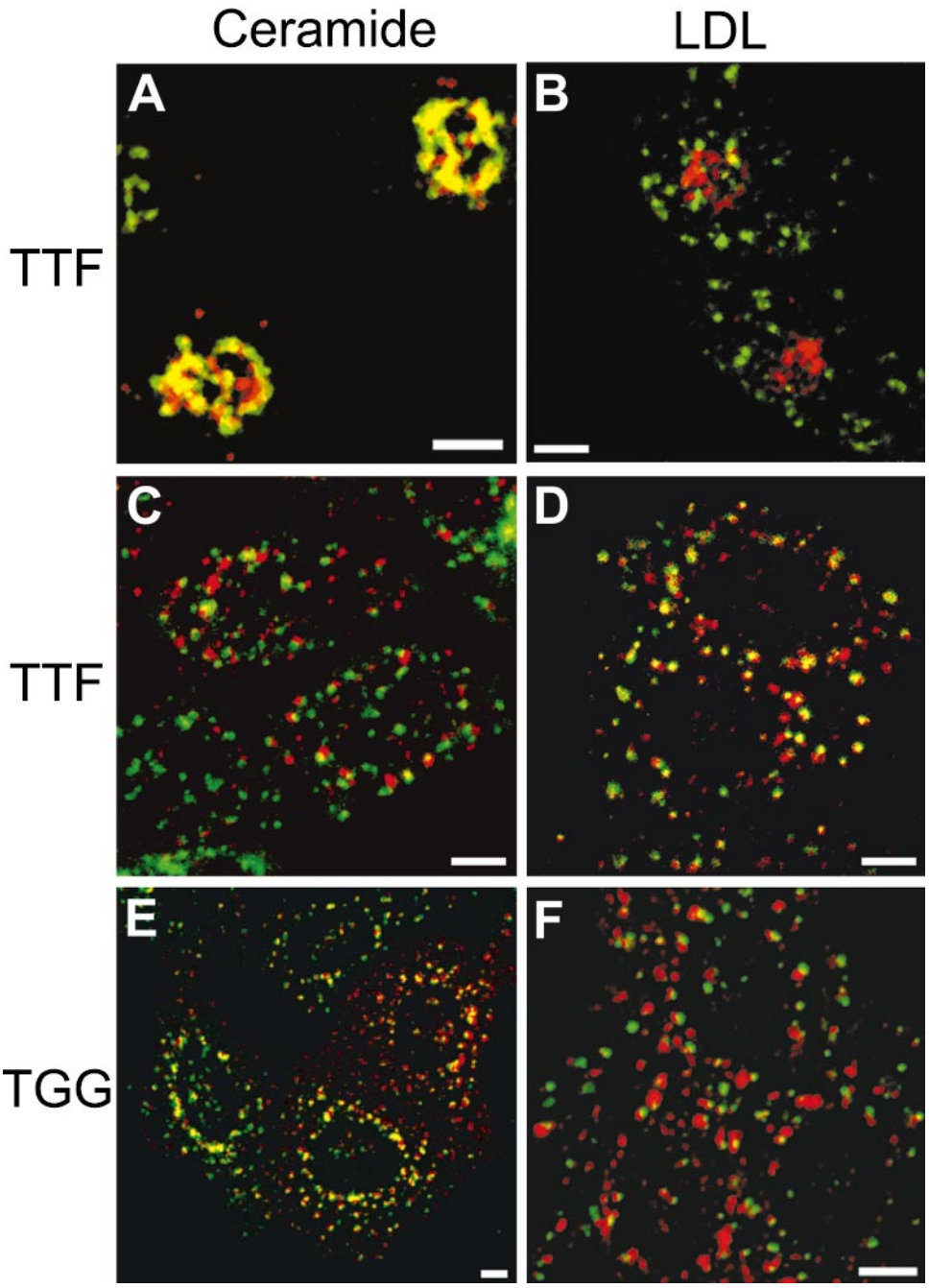

Figure 8. Nocodazole inhibits the postendocytic transport of Tac-furin to the TGN. TRVb-1/Tac-furin (A–D) and Tac-TGN38 (E and F) cells were pretreated with 0.1% DMSO (A and B) or 33 μM nocodazole in DMSO (C–F) as described in Materials and Methods. Cells were then incubated for 15 min with A488–anti-Tac (red; B, D, and F) plus DiI-LDL (green; B, D, and F) or Cy3–anti-Tac alone (red; A, C, and E), followed by a 45-min chase, maintaining the concentration of nocodazole throughout. After fixation, cells that received Cy3–anti-Tac were stained with NBD-C_6-ceramide (green; A, C, and E). Z-series confocal projections are shown. Pixels labeled with both fluorophores appear yellow. Bars, 10 μm.

nalized Tac-furin was delivered to the TGN only very inefficiently, instead remaining colocalized with LDL (Fig. 9, A–D). Note the nebulous appearance of the anti-Tac and LDL labeling in Fig. 9, A, C, and D; this pattern is presumably due to the effects of wortmannin on the morphology of endosomes. The appearance of Tac-TGN38 in the TGN also was reduced upon treatment with the drug, presumably due to slower transit of the chimera through the endocytic recycling pathway. However, significant colocalization of Cy3–anti-Tac and NBD-C_6-ceramide was apparent at the end of the 45-min chase (Fig. 9, E and F), increasing with a more prolonged chase (data not shown). Before delivery to the TGN, Tac-TGN38 remained colocalized with transferrin, and at no point was overlap with internalized LDL observed (data not shown). Given the reported activities of wortmannin and our own observations, the most straightforward conclusion is that Tac-furin trafficking is blocked from late endosomes to the TGN. This may represent a direct dependence of this transport event on PI3-kinase activity, or may be an indirect consequence of inhibiting the delivery of transport factors to late endosomes. Irrespective of the precise point of action of wortmannin, the absence of accumulation of Tac-TGN38 in LDL-containing endosomes under these conditions underscores the different pathways that these chimeras take in the endosomal system.

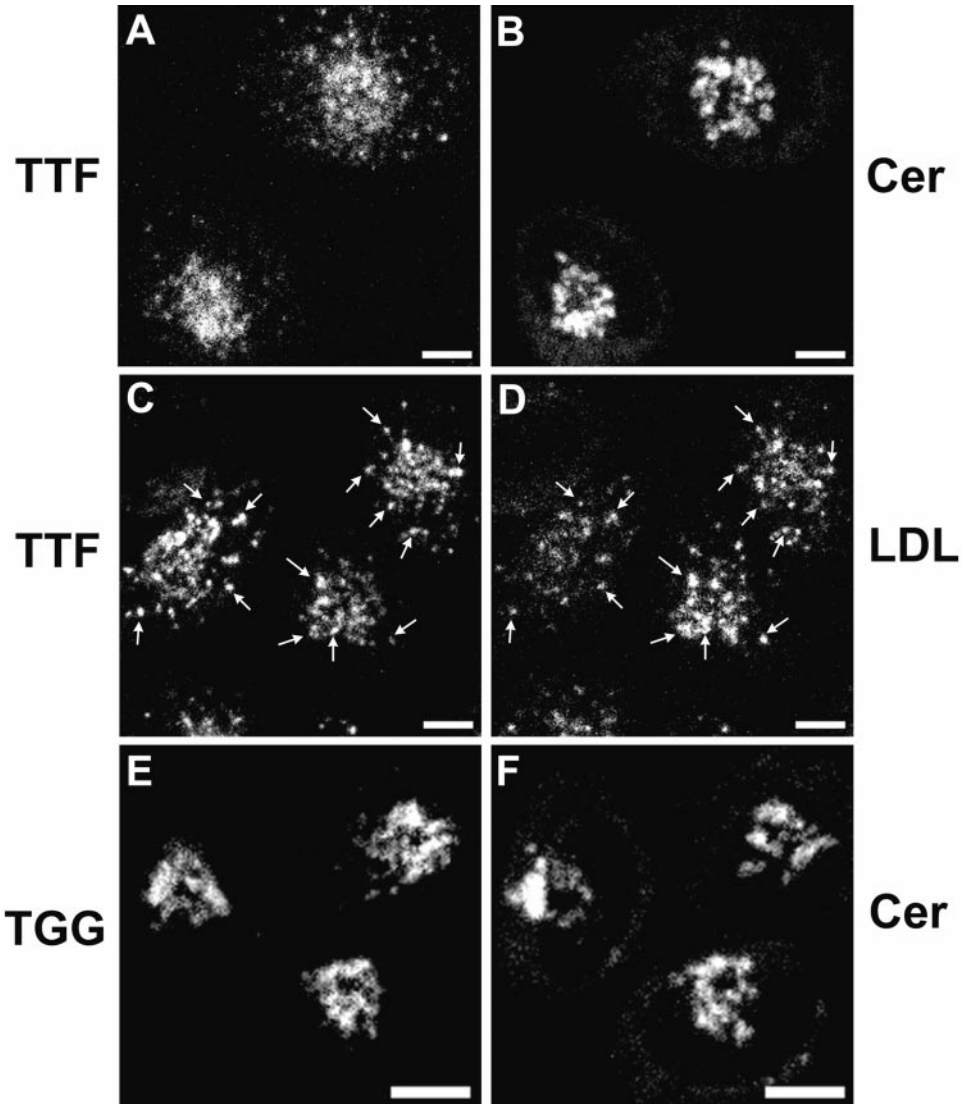

Figure 9. Wortmannin inhibits the delivery of internalized Tac-furin to the TGN, but has a milder effect on Tac-TGN38 transport. TRVb-1/Tac-furin (A–D) and Tac-TGN38 (E and F) cells were pretreated with 100 nM wortmannin as described in Materials and Methods. Cells then were incubated for 15 min with A488–anti-Tac (C) plus DiI-LDL (D) or Cy3–anti-Tac alone (A and E), followed by a 45-min chase, maintaining the concentration of wortmannin throughout. After fixation, cells that received Cy3–anti-Tac were stained with NBD-C_6-ceramide (Cer; B and F). Z-series confocal projections are shown. Arrows in C and D indicate some points of colocalization to assist the reader. Bars, 10 μm.

Discussion

Over the past several years, numerous reports have described the transport of certain membrane-associated proteins between the endosomal system and the secretory pathway, specifically the TGN. However, the exact route by which proteins are delivered to the TGN usually has not been specified. This is significant since the transport pathway determines where protein sorting must take place and also may suggest the mechanism of sorting. We demonstrated recently the postendocytic transport of a chimeric transmembrane protein, Tac-TGN38, to the TGN via the endocytic recycling pathway (Ghosh et al., 1998). In the present study, we have shown that another chimeric protein which is localized to the TGN, Tac-furin, is delivered there from late endosomes and does not traverse the recycling pathway. Therefore, CHO cells have at least two distinct mechanisms for endocytic transport of membrane proteins to the TGN (Fig. 10). Selective removal of Tac-TGN38 from the recycling pathway apparently occurs from the ERC. In contrast, Tac-furin is segregated from recycling proteins at an earlier step, the sorting endosome, allowing it to enter late endosomes. Furthermore, whereas Tac-TGN38 is removed from the recycling pathway and delivered to the TGN in an iterative manner, Tac-furin is segregated from late endosomes by a more efficient, single-pass mechanism, possibly in one concerted step.

The steady-state localization of a protein is determined by the slowest step in its trafficking. Irrespective of the transport itineraries and sorting mechanisms involved, both Tac-furin and Tac-TGN38 are localized to the TGN predominantly through their relatively slow rates of exit from that compartment. This is likely reflected in the rates of transport of the proteins from internal sites to the plasma membrane, which are slower than all other kinetic steps measured for each chimera. In the case of Tac-furin, the kinetics of exit from the cell appears to be independent of the transmembrane domain. However, this may not be the case for Tac-TGN38 (Ponnambalam et al., 1994). Tac-TGN38 exits the cell significantly slower than does Tac-furin (Ghosh et al., 1998), implying a possible role of the TGN38 transmembrane domain in retention of the chimera in the TGN.

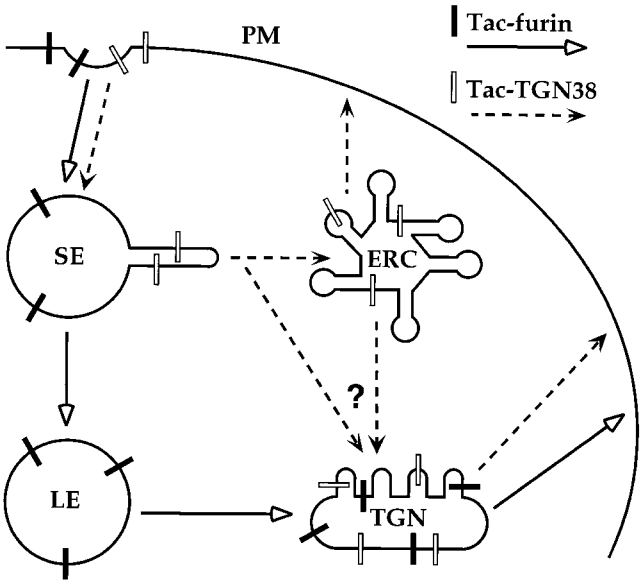

Figure 10. Model for the transport of Tac-TGN38 and Tac-furin from endosomes to the TGN. Both proteins are internalized from the plasma membrane (PM) and initially enter sorting endosomes (SE). Tac-furin is then delivered to late endosomes (LE), whereas Tac-TGN38 is transported to the ERC. The transport of Tac-furin from late endosomes to the TGN occurs before or coincident with the accumulation of CI-MPR in late endosomes (not depicted). The exact route that Tac-TGN38 follows from the recycling pathway to the TGN has not been determined, and may be from the ERC or from sorting endosomes, as indicated by "?" and the two converging arrows.

The two distinct endosomal pathways, which diverge at the level of the sorting endosome, indicate at least two sorting steps that are involved in transport to the TGN. Tac-TGN38 traverses the recycling pathway that is followed by the bulk of internalized membrane proteins in CHO cells in the absence of specific targeting. From some point along this pathway, Tac-TGN38 is then diverted for delivery to the TGN. This process must require a specific property of Tac-TGN38, such as an amino acid motif or selective partitioning into membrane domains due to the protein's physical characteristics. The cytoplasmic domain sequence, SDYQRL, appears to fulfill at least part of this sorting function (Bos et al., 1993; Humphrey et al., 1993; Wong and Hong, 1993; Ponnambalam et al., 1994). However, the SDYQRL motif is not sufficient for delivery from the ERC to the TGN (Johnson et al., 1996). Additionally, the similarity of the trafficking itinerary of the Shiga toxin B fragment, a soluble protein which binds to the glycolipid globotriaosylceramide (Lingwood, 1993), suggests that lipid-based sorting may also be critical along this pathway (Mallard et al., 1998). We have not determined the point of departure of Tac-TGN38 from the recycling pathway. The most likely possibility is that it exits from the recycling compartment, although a direct pathway from sorting endosomes cannot be excluded at present.

The itinerary followed by Tac-furin is now more completely described. This protein evades the endocytic recycling pathway, neither appearing in the ERC nor rapidly returning to the plasma membrane. Rather, Tac-furin transits from sorting endosomes to late endosomes, which must require high-fidelity, active sorting of Tac-furin at the sorting endosome. From late endosomes, Tac-furin is transported to the TGN, apparently before the accumulation of CI-MPR in late endosomes. This late endosome to TGN step may also require active sorting, or this may be the pathway taken by most membrane proteins that have accessed late endosomes, in the absence of a positive sorting signal. There is evidence that internalized membrane proteins such as the transferrin and LDL receptors may be transported from endosomes to the TGN at a low constitutive rate (Snider and Rogers, 1985; Green and Kelly, 1992; Bos et al., 1995). However, Tac-furin is delivered to the TGN with much higher efficiency than those receptors. Also, the transport of the cation-dependent mannose 6-phosphate receptor to the TGN requires an amino acid sequence in its cytoplasmic domain, and the receptor is degraded in lysosomes if this signal is disrupted (Rohrer et al., 1995). Whether dependent on a positive signal or not, the kinetics of separation of Tac-furin from LDL indicate that the mechanism for delivering Tac-furin to the TGN must be able to segregate a membrane-associated molecule from a soluble molecule very efficiently. This mechanism must also allow the efficient transport of growth factor receptors from late endosomes to lysosomes and not to the TGN. A series of reports has demonstrated the importance of an acidic cluster in the furin cytoplasmic domain for its delivery to the TGN (Jones et al., 1995; Schäfer et al., 1995; Takahashi et al., 1995; Voorhees et al., 1995), and specifically, the phosphorylation of serine residues within this region appears to be a major regulator of furin endosomal transport (Jones et al., 1995; Molloy et al., 1998), possibly directing furin into a rapid recycling pathway. Extensive and detailed analyses will be required to determine at which steps the acidic cluster, phosphorylation, and other putative sorting signals are required.

The different endosomal pathways followed by Tac-furin and Tac-TGN38 must require different sorting mechanisms, as supported by studies using nocodazole and wortmannin. The inhibition of Tac-furin transport by nocodazole is readily explained, since the chimera is delivered via late endosomes, and entry of endocytosed proteins into late endosomes is blocked by nocodazole. The absence of an effect on Tac-TGN38 transport is consistent with the properties of the endocytic recycling pathway, although it would not necessarily be predicted that a route linking the recycling pathway and the TGN would also be independent of microtubules. Our data also suggest that transport from late endosomes to the TGN depends on PI3 kinase activity since wortmannin apparently causes internalized Tac-furin to accumulate in late endosomes rather than in the TGN. This may reflect a general requirement for PI3 kinase in late endosome to TGN trafficking, or alternatively a specific role of PI3 kinase in the pathway that transports furin. Analyses of the effects of wortmannin treatment on endosome-to-TGN trafficking in other systems have yielded conflicting results (Nakajima and Pfeffer, 1997; Kundra and Kornfeld, 1998).

An extensive series of studies by Thomas and co-workers has revealed possible roles for a number of proteins,

including phosphofurin acidic cluster sorting protein 1 (PACS-1) (Wan et al., 1998), actin binding protein of 280 kD (Liu et al., 1997), and protein phosphatase 2A (Molloy et al., 1998), at various stages of furin transport to modulate either delivery to or retention in the TGN. Specifically, PACS-1 interacts with the furin acidic domain. PACS-1 also interacts with the MPR/IGF-II receptor but not with the primate TGN38 homologue, TGN46 (Wan et al., 1998), further supporting a role for PACS-1 in endosomal sorting. This interaction requires the phosphorylation of the furin cytoplasmic domain, which has also been shown to be a modulator of the intracellular distribution of furin (Jones et al., 1995; Molloy et al., 1998). The TGN38 cytoplasmic domain can also be phosphorylated in vitro with effects on its protein interactions (Zehavi-Feferman et al., 1995), and like furin the endocytic transport of TGN38 may be regulated by phosphorylation. However, the factors that are responsible for TGN38 sorting after internalization have not been conclusively identified. These may include as yet unidentified coat proteins and also may involve Rab11 and/or other regulatory GTPases. Careful examination of each step in endosomal transport will be necessary to assign these various species to their respective sites of action.

The authors thank Juan Bonifacino and Michael Marks for the Tac chimera plasmids, and Keith Stanley, George Banting, Yukio Ikehara, and Peter Lobel for antibodies used in these studies. We thank members of the Maxfield lab and Timothy McGraw for advice and suggestions, and members of the McGraw lab for extensive technical assistance. We are grateful to Anne Müsch, James Arden, and Sharron Lin (Weill Medical College of Cornell University, New York, NY) for critical reading of the manuscript. We also thank Dr. Xinwa Chang (Department of Medicine, Weill Medical College) for assistance with statistical analyses.

This work was supported by National Institutes of Health grant DK27083. W.G. Mallet was supported by a postdoctoral fellowship from the Pharmaceutical Research and Manufacturers of America Foundation.

Submitted: 29 March 1999
Revised: 28 May 1999
Accepted: 18 June 1999

References

Aniento, F., N. Emans, G. Griffiths, and J. Gruenberg. 1993. Cytoplasmic dynein-dependent vesicular transport from early to late endosomes. *J. Cell Biol.* 6:1373–1387.

Berger, E.G., P. Burger, A. Hille, and T. Bachi. 1995. Comparative localization of mannose-6-phosphate receptor with 2,6 sialyltransferase in HepG2 cells: an analysis by confocal double immunofluorescence microscopy. *Eur. J. Cell Biol.* 67:106–111.

Bomsel, M., R. Parton, S.A. Kuznetsov, T.A. Schroer, and J. Gruenberg. 1990. Microtubule and motor dependent fusion in vitro between apical and basolateral endocytic vesicle from MDCK cells. *Cell.* 62:719–731.

Bos, C.R., S.L. Shank, and M.D. Snider. 1995. Role of clathrin-coated vesicles in glycoprotein transport from the cell surface to the Golgi complex. *J. Biol. Chem*. 270:665–671.

Bos, K., C. Wraight, and K.K. Stanley. 1993. TGN38 is maintained in the *trans*-Golgi network by a tyrosine-containing motif in the cytoplasmic domain. *EMBO (Eur. Mol. Biol. Organ.) J.* 12:2219–2228.

Bosshart, H., J. Humphrey, E. Deignan, J. Davidson, J. Drazba, L. Yuan, V. Oorschot, P.J. Peters, and J.S. Bonifacino. 1994. The cytoplasmic domain mediates localization of furin to the trans-Golgi network en route to the endosomal/lysosomal system. *J. Cell Biol.* 126:1157–1172.

Brown, W.J., D.B. DeWald, S.D. Emr, H. Plutner, and W.E. Balch. 1995. Role for phosphatidylinositol 3-kinase in the sorting and transport of newly synthesized lysosomal enzymes in mammalian cells. *J. Cell Biol.* 130:781–796.

Chen, H.J., J. Remmler, J.C. Delaney, D.J. Messner, and P. Lobel. 1993. Mutational analysis of the cation-independent mannose 6-phosphate/insulin-like growth factor II receptor. *J. Cell Biol.* 268:22338–22346.

Dahms, N.M., P. Lobel, and S. Kornfeld. 1989. Mannose 6-phosphate receptors and lysosomal enzyme targeting. *J. Biol. Chem*. 264:12115–12118.

Davidson, H.W. 1995. Wortmannin causes mistargeting of procathepsin D. Evidence for the involvement of a phosphatidylinositol 3-kinase in vesicular transport to lysosomes. *J. Cell Biol.* 130:797–805.

Duncan, J.R., and S. Kornfeld. 1988. Intracellular movement of two mannose 6-phosphate receptors: return to the Golgi apparatus. *J. Cell Biol.* 106:617–628.

Dunn, K.W., and F.R. Maxfield. 1992. Delivery of ligands from sorting endosomes to late endosomes occurs by maturation of sorting endosomes. *J. Cell Biol.* 117:301–310.

Dunn, K.W., T.E. McGraw, and F.R. Maxfield. 1989. Iterative fractionation of recycling receptors from lysosomally destined ligands in an early sorting endosome. *J. Cell Biol.* 109:3303–3314.

Dunn, W.A., T.P. Connolly, and A.L. Hubbard. 1986. Receptor-mediated endocytosis of epidermal growth factor by rat hepatocytes: receptor pathway. *J. Cell Biol.* 102:24–36.

Geuze, H.J., J.W. Slot, G.J.A.M. Strous, A. Hasilik, and K. von Figura. 1984. Ultrastructural localization of the mannose 6-phosphate receptor in rat liver. *J. Cell Biol.* 98:2047–2054.

Ghosh, R.N., D.L. Gelman, and F.R. Maxfield. 1995. Quantification of low density lipoprotein and transferrin endocytic sorting in HEp2 cells using confocal microscopy. *J. Cell Sci.* 107:2177–2189.

Ghosh, R.N., W.G. Mallet, T.T. Soe, T.E. McGraw, and F.R. Maxfield. 1998. An endocytosed TGN38 chimeric protein is delivered to the TGN after trafficking through the endocytic recycling compartment in CHO cells. *J. Cell Biol.* 142:923–936.

Goldstein, J.L., M.S. Brown, R.G.W. Anderson, D.W. Russell, and W.J. Schneider. 1985. Receptor-mediated endocytosis: concepts emerging from the LDL receptor system. *Annu. Rev. Cell Biol.* 1:1–39.

Green, S.A., and R.B. Kelly. 1992. Low density lipoprotein receptor and cation-independent mannose 6-phosphate receptor are transported from the cell surface to the Golgi apparatus at equal rates in PC12 cells. *J. Cell Biol.* 117: 47–55.

Griffiths, G., B. Hoflack, K. Simons, I. Mellman, and S. Kornfeld. 1988. The mannose 6-phosphate receptor and the biogenesis of lysosomes. *Cell.* 52: 329–341.

Gruenberg, J., and F.R. Maxfield. 1995. Membrane transport in the endocytic pathway. *Curr. Opin. Cell Biol.* 7:552–563.

Gruenberg, J., G. Griffiths, and K.E. Howell. 1989. Characterization of the early endosome and putative endocytic carrier vesicles in vivo and with an assay of vesicle fusion in vitro. *J. Cell Biol.* 108:1301–1316.

Hopkins, C.R., and I.S. Trowbridge. 1983. Internalization and processing of transferrin and the transferrin receptor in human carcinoma A431 cells. *J. Cell Biol.* 97:508–521.

Humphrey, J.S., P.J. Peters, L.C. Yuan, and J.S. Bonifacino. 1993. Localization of TGN38 to the trans-Golgi network: involvement of a cytoplasmic tyrosine-containing sequence. *J. Cell Biol.* 120:1123–1135.

Jackle, S., E.A. Runquist, S. Miranda-Brady, and R.J. Havel. 1991. Trafficking of the epidermal growth factor receptor and transferrin in three hepatocytic endosomal fractions. *J. Biol. Chem.* 266:1396–1402.

Jin, M., and M.D. Snider. 1993. Role of microtubules in transferrin receptor transport from the cell surface to endosomes and the Golgi complex. *J. Biol. Chem*. 268:18390–18397.

Jin, M., G.G. Sahagian, and M.D. Snider. 1989. Transport of surface mannose 6-phosphate receptor to the Golgi complex in cultured human cells. *J. Biol. Chem*. 264:7675–7680.

Jing, S.Q., T. Spencer, K. Miller, C. Hopkins, and I.S. Trowbridge. 1990. Role of the human transferrin receptor cytoplasmic domain in endocytosis: localization of a specific signal sequence for internalization. *J. Cell Biol.* 110:283–294.

Johnson, A.O., R.N. Ghosh, K.W. Dunn, R. Garippa, J. Park, S. Mayor, F.R. Maxfield, and T.E. McGraw. 1996. Transferrin receptor containing the SDYQRL motif of TGN38 causes a reorganization of the recycling compartment but is not targeted to the TGN. *J. Cell Biol.* 135:1749–1762.

Jones, A.T., and M.J. Clague. 1995. Phosphatidylinositol 3-kinase activity is required for early endosome fusion. *Biochem. J.* 311:31–34.

Jones, B.G., L. Thomas, S.S. Molloy, C.D. Thulin, M.D. Fry, K.A. Walsh, and G. Thomas. 1995. Intracellular trafficking of furin is modulated by the phosphorylation state of a casein kinase II site in its cytoplasmic tail. *EMBO (Eur. Mol. Biol. Organ.) J.* 14:5869–5883.

Kleijmeer, M.J., S. Morkowski, J.M. Griffith, A.Y. Rudensky, and H.J. Geuze. 1997. Major histocompatibility complex class II compartments in human and mouse B lymphoblasts represent conventional endocytic compartments. *J. Cell Biol.* 139:639–649.

Kundra, R., and S. Kornfeld. 1998. Wortmannin retards the movement of the mannose 6-phosphate/insulin-like growth factor II receptor and its ligand out of endosomes. *J. Biol. Chem*. 273:3848–3853.

Ladinsky, M.S., and K.E. Howell. 1992. The trans-Golgi network can be dissected structurally and functionally from the cisternae of the Golgi complex by brefeldin A. *Eur. J. Cell Biol.* 59:92–105.

Ladinsky, M.S., D.N. Mastronarde, J.R. McIntosh, K.E. Howell, and L.A. Staehelin. 1999. Golgi structure in three dimensions: functional insights from the normal rat kidney cell. *J. Cell Biol.* 144:1135–1149.

Li, G., C. D'Souza-Schorey, M.A. Barbieri, R.L. Roberts, A. Klippel, L.T. Williams, and P.D. Stahl. 1995. Evidence for phosphatidylinositol 3-kinase as a regulator of endocytosis via activation of Rab5. *Proc. Natl. Acad. Sci. USA*. 92:10207–10211.

Lingwood, C.A. 1993. Verotoxins and their glycolipid receptors. *Adv. Lipid*

Res. 25:189–211.
Lippincott-Schwartz, J., L. Yuan, C. Tipper, M. Amherdt, L. Orci, and R.D. Klausner. 1991. Brefeldin A's effects on endosomes, lysosomes, and the TGN suggest a general mechanism for regulating organelle structure and membrane traffic. *Cell.* 67:601–616.
Liu, G., L. Thomas, R.A. Warren, C.A. Enns, C.C. Cunningham, J.H. Hartwig, and G. Thomas. 1997. Cytoskeletal protein ABP-280 directs the intracellular trafficking of furin and modulates proprotein processing in the endocytic pathway. *J. Cell Biol.* 139:1719–1733.
Luzio, J.P., B. Brake, G. Banting, K.E. Howell, P. Braghetta, and K.K. Stanley. 1990. Identification, sequencing and expression of an integral membrane protein of the *trans*-Golgi network (TGN38). *Biochem. J.* 270:97–102.
Mallard, F., C. Antony, D. Tenza, J. Salamero, B. Goud, and L. Johannes. 1998. Direct pathway from early/recycling endosomes to the Golgi apparatus revealed through the study of Shiga toxin B-fragment transport. *J. Cell Biol.* 143:973–990.
Martys, J.L., C. Wjasow, D.M. Gang, M.C. Kielian, T.E. McGraw, and J.M. Backer. 1996. Wortmannin-sensitive trafficking pathways in Chinese hamster ovary cells: differential effects on endocytosis and lysosomal sorting. *J. Biol. Chem.* 271:10953–10962.
Matter, K., J.A. Whitney, E.M. Yamamoto, and I. Mellman. 1993. Common signals control low density lipoprotein receptor sorting in endosomes and the Golgi complex of MDCK cells. *Cell.* 74:1053–1064.
Mayor, S., J.F. Presley, and F.R. Maxfield. 1993. Sorting of membrane components from endosomes and subsequent recycling to the cell surface occurs by a bulk flow process. *J. Cell Biol.* 121:1257–1269.
McGraw, T.E., L. Greenfield, and F.R. Maxfield. 1987. Functional expression of the human transferrin receptor cDNA in Chinese hamster ovary cells deficient in endogenous transferrin receptor. *J. Cell Biol.* 105:207–214.
McGraw, T.E., K.W. Dunn, and F.R. Maxfield. 1993. Isolation of a temperature-sensitive variant Chinese hamster ovary cell line with a morphologically altered endocytic recycling compartment. *J. Cell. Physiol.* 155:579–594.
Milgram, S.L., R.E. Mains, and B.A. Eipper. 1993. COOH-terminal signals mediate the trafficking of a peptide processing enzyme in endocrine cells. *J. Cell Biol.* 121:23–36.
Miller, K., J. Beardmore, H. Kanety, J. Schlessinger, and C.R. Hopkins. 1986. Localization of the epidermal growth factor (EGF) receptor within the endosome of EGF-stimulated epidermoid carcinoma (A431) cells. *J. Cell Biol.* 102:500–509.
Misumi, Y., K. Oda, T. Fujiwara, N. Takami, K. Tashiro, and Y. Ikehara. 1991. Functional expression of furin demonstrating its intracellular localization and endoprotease activity for processing of proalbumin and complement pro-C3. *J. Biol. Chem.* 266:16954–16959.
Molloy, S.S., L. Thomas, J.K. VanSlyke, P.E. Stenberg, and G. Thomas. 1994. Intracellular trafficking and activation of the furin proprotein convertase: localization to the TGN and recycling from the cell surface. *EMBO (Eur. Mol. Biol. Organ.) J.* 13:18–33.
Molloy, S.S., L. Thomas, C. Kamibayashi, M.C. Mumby, and G. Thomas. 1998. Regulation of endosome sorting by a specific PP2A isoform. *J. Cell Biol.* 142:1399–1411.
Mostov, K.E., and M.H. Cardone. 1995. Regulation of protein traffic in polarized epithelial cells. *Bioessays.* 17:129–138.
Mukherjee, S.M., R.N. Ghosh, and F.R. Maxfield. 1997. Endocytosis. *Physiol. Rev.* 77:759–803.
Nakajima, Y., and S.R. Pfeffer. 1997. Phosphatidylinositol 3-kinase is not required for recycling of mannose 6-phosphate receptors from late endosomes to the trans-Golgi network. *Mol. Biol. Cell.* 8:577–582.
Pagano, R.E., M.A. Sepanski, and O.C. Martin. 1989. Molecular trapping of a fluorescent ceramide analogue at the Golgi apparatus of fixed cells: interaction with endogenous lipids provides a trans-Golgi marker for both light and electron microscopy. *J. Cell Biol.* 109:2067–2079.
Pitas, R.E., T.L. Innerarity, J.N. Weinstein, and R.W. Mahley. 1981. Acetoacetylated lipoproteins used to distinguish fibroblasts from macrophages *in vitro* by fluorescence microscopy. *Arteriosclerosis.* 1:177–185.
Ponnambalam, S., C. Rabouille, J.P. Luzio, T. Nilsson, and G. Warren. 1994. The TGN38 glycoprotein contains two non-overlapping signals that mediate localization to the trans-Golgi network. *J. Cell Biol.* 125:253–268.
Reaves, B., M. Horn, and G. Banting. 1993. TGN38/41 recycles between the cell surface and the TGN: Brefeldin A affects its rate of return to the TGN. *Mol. Biol. Cell.* 4:93–105.
Rogalski, A.A., and S.J. Singer. 1984. Associations of elements of the Golgi apparatus with microtubules. *J. Cell Biol.* 99:1092–1100.
Rohrer, J., A. Schweizer, K.F. Johnson, and S. Kornfeld. 1995. A determinant in the cytoplasmic tail of the cation-dependent mannose 6-phosphate receptor prevents trafficking to lysosomes. *J. Cell Biol.* 130:1297–1306.
Sakai, T., S. Yamashina, and S. Ohnishi. 1991. Microtubule-disrupting drugs blocked delivery of endocytosed transferrin to the cytocenter, but did not affect return of transferrin to plasma membrane. *J. Biochem. (Tokyo).* 109: 528–533.
Salzman, N.H., and F.R. Maxfield. 1988. Intracellular fusion of sequentially formed endocytic compartments. *J. Cell Biol.* 106:1083–1091.
Salzman, N.H., and F.R. Maxfield. 1989. Fusion accessibility of endocytic compartments along the recycling and lysosomal endocytic pathways in intact cells. *J. Cell Biol.* 109:2097–2104.
Schäfer, W., A. Stroh, S. Berghöfer, J. Seiler, M. Vey, M.-L. Kruse, H.F. Kern, H.-D. Klenk, and W. Garten. 1995. Two independent targeting signals in the cytoplasmic domain determine *trans*-Golgi network localization and endosomal trafficking of the proprotein convertase furin. *EMBO (Eur. Mol. Biol. Organ.) J.* 14:2424–2435.
Shpetner, H., M. Joly, D. Hartley, and S. Corvera. 1996. Potential sites of PI-3 kinase function in the endocytic pathway revealed by the PI-3 kinase inhibitor, wortmannin. *J. Cell Biol.* 132:595–605.
Snider, M.D., and O.C. Rogers. 1985. Intracellular movement of cell surface receptors after endocytosis: resialylation of asialo-transferrin receptor in human erythroleukemia cells. *J. Cell Biol.* 100:826–834.
Spiro, D.J., W. Boll, T. Kirchhausen, and M. Wessling-Resnick. 1996. Wortmannin alters the transferrin receptor endocytic pathway in vivo and in vitro. *Mol. Biol. Cell.* 7:355–367.
Takahashi, S., T. Nakagawa, T. Banno, T. Watanabe, K. Murakami, and K. Nakayama. 1995. Localization of furin to the *trans*-Golgi network and recycling from the cell surface involves Ser and Tyr residues within the cytoplasmic domain. *J. Biol. Chem.* 270:28397–28401.
Takeuchi, Y., M. Yanagishita, and V.C. Hascall. 1992. Recycling of transferrin receptor and heparan sulfate proteoglycans in a rat parathyroid cell line. *J. Biol. Chem.* 267:14685–14690.
Ullrich, O., S. Reinsch, S. Úrbe, M. Zerial, and R.G. Parton. 1996. Rab11 regulates recycling through the pericentriolar recycling endosome. *J. Cell Biol.* 135:913–924.
Úrbe, S., L.A. Huber, M. Zerial, S.A. Tooze, and R.G. Parton. 1993. Rab11, a small GTPase associated with both constitutive and regulated secretory pathways in PC12 cells. *FEBS Lett.* 334:175–182.
Varlamov, O., and L.D. Fricker. 1998. Intracellular trafficking of metallocarboxypeptidase D in AtT-20 cells: localization to the *trans*-Golgi network and recycling from the cell surface. *J. Cell Sci.* 111:877–885.
Voorhees, P., E. Deignan, E. van Donselaar, J. Humphrey, M.S. Marks, P.J. Peters, and J.S. Bonifacino. 1995. An acidic sequence within the cytoplasmic domain of furin functions as a determinant of *trans*-Golgi network localization and internalization from the cell surface. *EMBO (Eur. Mol. Biol. Organ.) J.* 14:4961–4975.
Wan, L., S.S. Molloy, L. Thomas, G. Liu, Y. Xiang, S.L. Rybak, and G. Thomas. 1998. PACS-1 defines a novel gene family of cytosolic sorting proteins required for *trans*-Golgi network localization. *Cell.* 94:205–216.
Wilde, A., B. Reaves, and G. Banting. 1992. Epitope mapping of two isoforms of a trans Golgi network specific integral membrane protein TGN38/41. *FEBS Lett.* 313:235–238.
Wiley, H.S., and D.D. Cunningham. 1982. The endocytic rate constant. *J. Biol. Chem.* 257:4222–4229.
Willingham, M.C., I.H. Pastan, and G.G. Sahagian. 1983. Ultrastructural immunocytochemical localization of the phosphomannosyl receptor in Chinese hamster ovary (CHO) cells. *J. Histochem. Cytochem.* 31:1–11.
Wolins, N., H. Bosshart, H. Küster, and J.S. Bonifacino. 1997. Aggregation as a determinant of protein fate in post-Golgi compartments: role of the luminal domain of furin in lysosomal targeting. *J. Cell Biol.* 139:1735–1745.
Wong, S.H., and W. Hong. 1993. The SxYQRL sequence in the cytoplasmic domain of TGN38 plays a major role in *trans*-Golgi network localization. *J. Biol. Chem.* 268:22853–22862.
Yamashiro, D.J., B. Tycko, S.R. Fluss, and F.R. Maxfield. 1984. Segregation of transferrin to a mildly acidic (pH 6.5) para-Golgi compartment in the recycling pathway. *Cell.* 37:789–800.
Zehavi-Feferman, R., J.W. Burgess, and K.K. Stanley. 1995. Control of p62 binding to TGN38/41 by phosphorylation. *FEBS Lett.* 368:122–124.